A&A 470, 557–570 (2007)
DOI: 10.1051/0004-6361:20077732

Astronomy & Astrophysics

Elusive AGN in the *XMM-Newton* bright serendipitous survey⋆,⋆⋆

A. Caccianiga[1], P. Severgnini[1], R. Della Ceca[1], T. Maccacaro[1], F. J. Carrera[2], and M. J. Page[3]

[1] INAF - Osservatorio Astronomico di Brera, via Brera 28, 20121 Milan, Italy
e-mail: [alessandro.caccianiga;paola.severgnini;roberto.dellaceca;tommaso.maccacaro]@brera.inaf.it
[2] Instituto de Física de Cantabria (CSIC-UC), Avenida de los Castros, 39005 Santander, Spain
e-mail: carreraf@ifca.unican.es
[3] Mullard Space Science Laboratory, University College London, Holmbury St. Mary, Dorking RH5 6NT, Surrey, UK
e-mail: mjp@mssl.ucl.ac.uk

Received 27 April 2007 / Accepted 11 May 2007

ABSTRACT

Context. Optical follow-up of X-ray selected sources finds a significant fraction of "optically dull" sources characterized by optical spectra without obvious signature of AGN activity. In many cases, however, the presence of an AGN is inferred from other diagnostics (e.g. the X-ray properties). Understanding and accounting for this "elusiveness" is mandatory for a reliable study of the AGN physical and statistical properties.
Aims. We investigate here the nature of all the sources (35 in total) in the XMM-Newton bright serendipitous survey (which is 86% optically identified) showing an optical spectrum dominated by the light from the host galaxy with no evidence (or little evidence) for the presence of an AGN.
Methods. We use the X-ray spectral analysis to assess the presence of an AGN in these sources and to characterize its properties.
Results. We detect AGN activity in 33 out of 35 sources. The remaining 2 sources are the ones with the lowest X-ray luminosity in the sample ($L_{[2-10\ \mathrm{keV}]} < 10^{41}$ erg s^{-1}) and their X-ray emission could be produced within the host galaxy. We find that the "recognition problem" for AGN is very critical in the low-luminosity regime (at least 60% of the AGN with $L_{[2-10\ \mathrm{keV}]} < 10^{43}$ erg s^{-1} are elusive) becoming negligible for high X-ray luminosities (∼1.5% of elusive AGN with $L_{[2-10\ \mathrm{keV}]} > 10^{44}$ erg s^{-1}). This problem affects mostly absorbed AGN (∼40% of type 2 AGN in the survey are elusive) but also a significant fraction of unabsorbed AGN (8%).
Conclusions. We find that the simplest explanations of why these 33 (or most of them) AGNs are elusive are two: at low X-ray luminosities ($<10^{43}$ erg s^{-1}) the most important reason is the intrinsically low AGN/galaxy contrast (optical dilution) while at high luminosities ($>10^{44}$ erg s^{-1}) it is due to the optical absorption (in the Compton-thin regime, i.e. $N_{\mathrm{H}} < 10^{24}$ cm^{-2}). Alternative hypotheses, like the presence of Compton-thick sources, BL Lac objects or "non-standard" AGN (e.g. with $\alpha_{\mathrm{OX}} < 1$ or with weak/absorbed Narrow Line Region) are not supported by the data although we cannot exclude the presence in the sample of a few sources of these types.

Key words. galaxies: active – galaxies: nuclei – X-ray: galaxies – surveys

1. Introduction

A great wealth of information on X-ray selected sources is usually obtained from the analysis of their optical counterparts. Optical spectroscopy, in particular, represents the fundamental step to determine not only the distance (for extragalactic objects) but also a classification of the source. Whether the observed X-ray emission is attributed to a nuclear activity or not is often inferred from the spectral properties of its optical counterpart. Also the characterization of the "AGN type" (type 1, type 2, BL Lac object, ...) is mostly based on the information derived from the spectroscopic analysis. This "optical step", while often necessary due to the difficulty of obtaining this information directly from the X-ray data, can be potentially problematic when the optical strength of the AGN, for whatever reason, is not expected to dominate on the host-galaxy emission. This "recognition problem" is obviously critical for intrinsically featureless AGN, like the BL Lac objects, as pointed out by Browne & Marchã (1993), but it can be important also for emission line AGN. Indeed, the presence of absorption or an intrinsic weakness of the AGN (or a combination of the two) may hide the AGN activity behind the normal star-light of the host galaxy also in emission line sources. The optical elusiveness (or "dullness") of some X-ray selected AGN is well known since the early surveys made with the *Einstein* Observatory and has been recently pointed out as a critical problem when studying the nature of the X-ray background and, in general, when studying the nature of X-ray selected sources (e.g. Elvis et al. 1981; Maccacaro et al. 1987; Griffiths et al. 1995; Comastri et al. 2002; Severgnini et al. 2003; Yuan & Narayan 2004; Georgantopoulos & Georgakakis 2005; Rigby et al. 2006). Optical elusiveness is often associated to the existence of X-ray sources with relatively large X-ray luminosity ($>10^{42}$ erg s^{-1}) and an early-type galaxy optical spectrum (the so-called XBONG, for X-ray Bright Optically Normal Galaxies). As discussed by Maiolino et al. (2003), however, the correct definition of "optically elusive AGN" should include also sources with starburst or LINER optical spectrum, coupled to

⋆ Based on observations collected at the Telescopio Nazionale Galileo (TNG) and at the European Southern Observatory (ESO), La Silla, Chile and on observations obtained with *XMM-Newton*, an ESA science mission with instruments and contributions directly funded by ESA Member States and the USA (NASA).
⋆⋆ Appendices A and B are only available in electronic form at http://www.aanda.org

an unusually (for these types of objects) "high" X-ray luminosity and not restricted just to the sources with an early-type galaxy spectrum. Indeed, "hard" (2–10 keV) X-ray observations have often revealed the presence of an "hidden" AGN in sources optically classified as starburst galaxies (e.g. Della Ceca et al. 2001; Franceschini et al. 2003).

Apart from making the detection of nuclear activity difficult, a low AGN/host-galaxy relative strength in the optical band may also create many problems for the correct definition of the AGN type. For instance, sources whose optical spectrum is characterized by an early-type galaxy spectrum plus a broad Hα line are generically classified as AGN, but establishing the amount of optical absorption is not trivial: a broad Hα line is observed both in "classical" Seyfert 1, completely unaffected by optical absorption, and in Seyfert 1.8/1.9, where a significant level of absorption is expected ($A_V \sim 2$–3 mag) and that are often grouped with Seyfert 2 in the statistical analysis of AGN samples (e.g. Maiolino & Rieke 1995).

The impact of a systematic mis-classification of elusive AGN on the statistical analysis of a sample of X-ray selected AGN can be significant as the percentage of these sources can be very high (40–60% in deep surveys, e.g. Hornschemeier et al. 2001).

In this paper we address this problem by analyzing in detail the properties of 35 X-ray sources selected in the *XMM-Newton* Bright Serendipitous survey (XBS, Della Ceca et al. 2004) that show an optical spectrum which is dominated by the host-galaxy light with no or little evidence of the presence of an AGN. These 35 objects are selected from a statistically well defined survey with a high identification level (∼86%). For this reason, once the nature of these sources has been established, we will be in the position of making firm statements on the statistical importance of the optical recognition of AGN at different X-ray luminosities and for different classes of objects.

After the definition of the sample (Sect. 2) we use the X-ray data to assess the presence of an AGN in these 35 objects (Sect. 3) and we study (Sect. 4) the possible reasons for their optical elusiveness using a simple spectral model. We summarize the conclusions in Sect. 5. Throughout this paper $H_0 = 65\ \mathrm{km\,s^{-1}\ Mpc^{-1}}$, $\Omega_\Lambda = 0.7$ and $\Omega_\mathrm{M} = 0.3$ are assumed.

2. Optically elusive AGN candidates in the XBS survey

The *XMM-Newton* Bright Serendipitous Survey (XBS survey, Della Ceca et al. 2004) is a wide-angle (28 sq. deg) high Galactic latitude ($|b| > 20$ deg) survey based on the *XMM-Newton* archival data. It is composed by two samples both flux-limited ($\sim 7 \times 10^{-14}$ erg s^{-1} cm^{-2}) in two separate energy bands: the 0.5–4.5 keV band (the BSS sample) and the 4.5–7.5 keV band (the "hard" HBSS sample). A total of 237 (211 for the HBSS sample) independent fields have been used to select 400 sources, 389 belonging to the BSS sample and 67 to the HBSS sample (56 sources are in common). The details on the fields selection strategy, the sources selection criteria and the general properties of the 400 objects are discussed in Della Ceca et al. (2004).

To date, the spectroscopic identification has been nearly completed and 86% of the 400 sources have been already spectroscopically observed and classified. The results will be presented in Caccianiga et al. (2007, in prep.).

A significant number of sources in the XBS survey is characterized by the presence, in the optical spectrum, of a important contamination from the host galaxy star-light: for instance in about 80 objects (i.e. ∼27% of the extragalactic objects) we detect a sharp 4000 Å break (>20%), a clear indication that the continuum is highly contaminated by the star-light from the host galaxy. In some cases, besides the star-light continuum, we detect broad and/or narrow emission lines that allow to detect and correctly classify the X-ray source as AGN. But in a significant number of objects (20) the optical spectrum does not offer a direct convincing evidence for the presence of an AGN. These objects are either optically classified as galaxies with an early-type spectrum (XBONG, 11 sources) or they can be classified as HII-region/starburst galaxies or LINERS on the basis of the diagnostic diagrams (e.g. Veilleux & Osterbrock 1987, 9 objects). We note that a LINER spectrum does not necessarily imply the presence of an AGN (e.g. see discussion in Maiolino et al. 2003).

In some other cases (10 objects), a broad (>1000–2000 km s^{-1}) Hα is possibly present but most of the remaining emission lines (in particular the Hβ emission line) are not detected. Even if the presence of an AGN in these sources is suggested by the detection of a broad Hα, we group also these objects among the "elusive" AGNs. The reason is twofold: first, the correct estimate of the Hα line width is not trivial in these objects given the relative weakness of the line and the presence of the two [NII] emission lines that are often blended with the Hα. This means that the optical evidence for an AGN in these sources is often questionable. Second, this kind of object, if put at larger redshift ($z > 0.3$–0.4) and observed with the usual wavelength coverage (up to ∼8500–9000 Å) would appear as "normal ellipticals" and would be classified as XBONGs. Indeed, most of the sources classified as XBONGs in deep X-ray surveys (and 4 out 11 XBONG in the XBS survey) do not have optical spectra covering the Hα region and, therefore, it is not possible to apply a classification criterion based on the Hα properties. For consistency with the literature it is therefore useful to classify also these sources as "elusive" AGN.

Finally, 5 additional sources show the line [OIII]λ5007 Å which can be suggestive for the presence of an AGN, but no Hβ is detected, thus preventing a firm classification of the source. Again, the classification as AGN and its characterization is difficult also in these objects due to the host-galaxy light in the optical spectrum.

We call *optically elusive AGN candidates* the 35 sources (20+10+5) for which no-evidence or little evidence for the presence of an AGN can be inferred from the optical spectrum. The reason why we believe that most of the sources in this group are actually hiding an AGN is that the large majority of them have an (observed, i.e. not corrected for absorption) X-ray luminosity larger than 10^{42} erg s^{-1} cm^{-2} and an X-ray-to-optical flux ratio (using the observed 2–10 keV flux and R magnitude) between 0.1 and 10 (see Fig. 1), something which is strongly indicative of the presence of an AGN (Fiore et al. 2003).

In Table 1 the optically elusive AGN candidates are listed together with a short description of their optical spectrum (Col. 4), the redshift (Col. 5), the magnitude[1] (Col. 6) and the reference to the optical spectrum (Col. 7). The optical spectra of the 30 objects observed in our own spectroscopy plus an unpublished spectrum (XBSJ163332.3+570520) taken from the RIXOS project (Mason et al. 2000) are reported in Fig. 2. More details on some of these sources are discussed in Appendix B.

[1] Most of the magnitudes are taken from APM (Automated Plate Measuring machine facility `www.ast.cam.ac.uk/~apmcat/`). Since APM magnitudes of bright and extended sources can be systematically underestimated we have applied, in these cases, a correction discussed in Marchã et al. (2001).

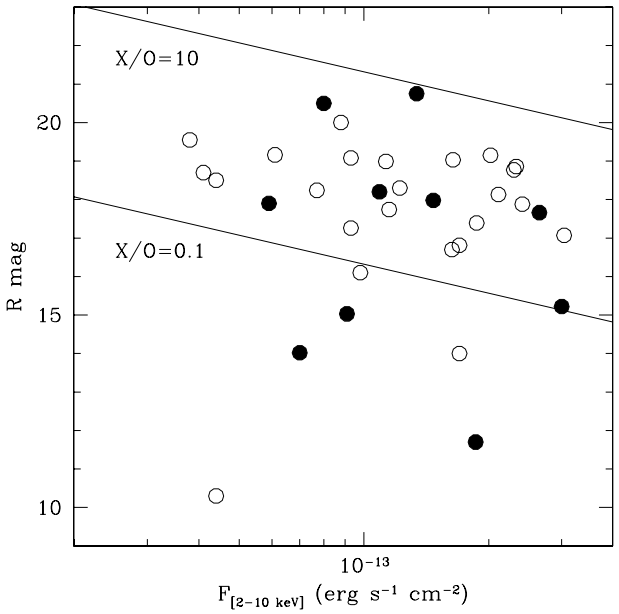

Fig. 1. The magnitude/X-ray flux of the 35 elusive AGN candidates discussed in this paper. Filled circles represent the objects with an early-type spectrum.

3. X-ray spectral analysis

Given the difficulty (or the impossibility) of finding from the optical spectra direct and strong evidence for the presence of an AGN in the 35 sources discussed here, we use as starting point the X-ray data, that are available, by definition, for the entire group of objects. The X-ray data have the advantage with respect to the optical band of being less affected by the presence of non-nuclear emission so that the AGN/galaxy contrast is expected to be larger. This is particularly true when the X-ray data cover hard energies (>2 keV), as in the case of *XMM-Newton* data.

For 4 sources (XBSJ021822.2−050615, XBSJ031859.2−441627, XBSJ075117.9+180856 and XBSJ231546.5−590313) a *XMM-Newton* analysis has been already presented and discussed in Severgnini et al. (2003) (the former three sources) or in Franceschini et al. (2003) (the latter one) and, therefore, we keep the results from that analysis and report the numbers published in these two papers. An additional source (XBSJ012654.3+191246), a radio-loud source, has been already presented in Galbiati et al. (2005) but we have re-done the X-ray analysis using a different model.

For the X-ray spectral analysis of the remaining 31 sources we have considered all the epic detectors available for each source. In general, data from the 2 MOS cameras are always available, while the epic-pn is missing in 8 cases (detector not available or sources outside the field-of-view or under a CCD gap).

Before the extraction of the spectra we have removed the time intervals with a high background. The source extraction region is a circular one with a radius of 20″–30″, depending on the source off-axis distance. The background is extracted in a nearby source-free circular region of radius ∼2 times larger than the one used for the source. The data from the two MOS cameras have been combined after the extraction if the same blocking filter is used. MOS and pn data have been re-binned in order to have at least 15–20 counts per channel, depending on the brightness of the source.

We have used XSPEC (ver. 11.3.1) to perform a simultaneous fitting analysis of the MOS and pn data leaving the relative normalization free to vary. All the relevant quantities (fluxes, luminosities, ...) are computed using the MOS normalization (or MOS2 if the two MOS cameras are not combined together).

As usual, errors are given at the 90% confidence level for one interesting parameter ($\Delta\chi^2 = 2.71$).

We have always tried to fit the spectra both with a simple absorbed power-law model and with a thermal model (Mekal). The reason for choosing these two models is that we expect most of the sources analysed here to contain an AGN (either absorbed or unabsorbed) or, alternatively, that the observed X-ray emission is due to the galaxy or to a group/cluster of galaxies.

Power-law model. In the large majority of cases (27/35) a simple absorbed power-law model offers an acceptable description of the data. In 3 additional cases this model is unable to give a good fit, leaving significant residuals in the highest energy bins. In these cases also the thermal model is rejected. We find that a better fit is obtained with a more complex model, composed by two power-laws, one absorbed and one unabsorbed, having the same spectral index (*leaky absorbed power-law model*). This model has different physical interpretations. For instance, the leaky-model can represent the physical case where the X-ray primary source is observed both directly, through a cold absorbing medium, and scattered (not absorbed) by a warm, highly ionized gas located outside the absorbing medium. The *leaky absorbed power-law model* has been used by Franceschini et al. (2003) also in the case of the source XBSJ231546.5−590313 (IRAS 23128−5919) with the addition of a thermal component ($kT \sim 0.65$ keV).

In 4 other cases a thermal model (black-body or Mekal model) is required in addition to the power-law component, to better describe the low-energy part of the spectrum.

When the power-law model is statistically acceptable but the counts are too few (<100 counts) to well constrain both the absorption and the spectral index, we have decided to fix the spectral index to $\Gamma = 1.9$, which is the mean value observed in the XBS survey of AGN (see Caccianiga et al. 2004; and Della Ceca et al. 2007, in prep), to better constrain the absorption. In one further case (XBSJ142741.8+423335) we have decided to fix the value of Γ to 1.9 since the best-fit Γ is much flatter (1.1) than the flattest Γ observed among the unabsorbed AGN of the XBS survey (∼1.5) and we suspect that the combination absorption/relatively low-statistics leads to an underestimate of both Γ and $N_{\rm H}$. By fixing the value of Γ to 1.9 we find an absorption which is ∼70% higher than the one estimated by leaving Γ free to vary. In both cases, however, the presence of a relatively large absorption ($>2 \times 10^{22}$ cm^{-2}) is confirmed, i.e. the classification of the source as "absorbed AGN" (see below) does not depend on the assumption on Γ.

Thermal model. As a first step, we consider acceptable a thermal model (Mekal) which gives a statistically significant fit (χ^2 probability larger than 5%) with values of a temperature below 10 keV. Usually the thermal model is statistically rejected for "flat" spectra, i.e. those well fitted by flat ($\Gamma < 1.7$) and/or absorbed power-laws. Then we have further analysed the cases where a thermal model is statistically acceptable to decide whether the best-fit temperature is physical or not, considered the X-ray luminosity of the source. It is well known, in fact, that in both clusters of galaxies and "normal" elliptical galaxies, there is relationship between the host-gas temperature and its X-ray luminosity (e.g. Fukazawa et al. 2004, and references therein). Using the relationship between these two quantities reported in Fukazawa et al. (2004) for a compilation of

Table 1. Optical properties of the diluted AGN candidates.

Name	Sample	Optical position (J2000)	Spectral description	z	mag	Reference
XBSJ000532.7+200716	bs	00 05 32.84 +20 07 17.4	early type spectrum	0.119	17.90 [1]	obs
XBSJ012540.2+015752	bs	01 25 40.36 +01 57 53.8	narrow emission lines	0.123	17.26 [1]	obs
XBSJ012654.3+191246	bs	01 26 54.45 +19 12 52.5	early type spectrum	0.043	13.70 [2]	obs
XBSJ013944.0–674909	bs, hbs	01 39 43.70 –67 49 08.1	broad Hα	0.104	17.74 [1]	obs
XBSJ014109.9–675639	bs	01 41 09.53 –67 56 38.7	broad Hα	0.226	19.15 [1]	obs
XBSJ014227.0+133453	bs	01 42 27.31 +13 34 53.1	narrow emission lines	0.275	19.08 [1]	obs
XBSJ021822.2–050615	hbs	02 18 22.16 –05 06 14.4	early type spectrum	0.044	15.22 [2]	obs
XBSJ025645.4+000031	bs	02 56 45.29 +00 00 33.2	broad Hα?	0.359	19.16 [1]	obs
XBSJ031859.2–441627	bs, hbs	03 18 59.46 –44 16 26.4	broad Hα	0.140	16.70 [2]	obs
XBSJ043448.3–775329	bs	04 34 47.78 –77 53 28.3	early type spectrum	0.097	17.66 [1]	obs
XBSJ050453.4–284532	bs	05 04 53.35 –28 45 31.0	[OIII] and no Hβ	0.204	18.99 [2]	obs
XBSJ051822.6+793208	bs	05 18 22.55 +79 32 09.8	early type spectrum	0.053	15.03 [1]	obs
XBSJ052116.2–252957	bs	05 21 16.08 –25 29 58.3	broad Hα?	0.332	19.55 [2]	obs
XBSJ052128.9–253032	hbs	05 21 29.04 –25 30 32.3	early type spectrum	0.588	20.75 [2]	obs
XBSJ075117.9+180856	bs	07 51 17.96 +18 08 56.0	broad Hα	0.255	19.03 [1]	obs
XBSJ083737.0+255151	bs, hbs	08 37 37.04 +25 51 51.6	narrow emission lines	0.105	17.07 [1]	obs
XBSJ090729.1+620824	bs	09 07 29.30 +62 08 27.0	early type spectrum	0.388	20.50 [3]	obs
XBSJ094526.2–085006	bs	09 45 26.25 –08 50 05.9	broad Hα	0.314	18.24 [2]	obs
XBSJ100032.5+553626	bs	10 00 32.29 +55 36 30.6	narrow emission lines	0.216	17.88 [2]	1
XBSJ101843.0+413515	bs	10 18 43.16 +41 35 16.5	broad Hα?	0.084	16.10 [1]	obs
XBSJ111654.8+180304	bs	11 16 54.72 +18 03 05.9	narrow emission lines	0.003	10.30 [2]	2
XBSJ112026.7+431520	hbs	11 20 26.62 +43 15 18.2	broad Hα	0.146	17.39 [1]	obs
XBSJ122017.5+752217	bs	12 20 17.76 +75 22 15.2	early type spectrum	0.006	11.70 [2]	3
XBSJ133942.6–315004	bs, hbs	13 39 42.47 –31 50 03.0	broad Hα	0.114	16.81 [1]	obs
XBSJ134656.7+580315	hbs	13 46 56.75 +58 03 15.7	early type spectrum	0.373	17.98 [1]	obs
XBSJ140100.0–110942	bs	14 00 59.93 –11 09 40.8	narrow emission lines	0.164	18.70 [2]	obs
XBSJ142741.8+423335	hbs	14 27 41.62 +42 33 38.1	strong [OIII] and no Hβ	0.142	18.13 [1]	obs
XBSJ143835.1+642928	bs, hbs	14 38 34.72 +64 29 31.1	narrow emission lines	0.118	18.86 [1]	obs
XBSJ143911.2+640526	hbs	14 39 10.72 +64 05 28.9	early type spectrum	0.113	18.20 [1]	obs
XBSJ161820.7+124116	hbs	16 18 20.82 +12 41 15.4	strong [OIII] and no Hβ	0.361	20.00 [3]	obs
XBSJ163332.3+570520	bs	16 33 31.94 +57 05 19.9	[OIII] and no Hβ	0.386	18.50 [1]	4
XBSJ193248.8–723355	bs, hbs	19 32 48.56 –72 33 53.0	narrow emission lines	0.287	18.77 [1]	obs
XBSJ230401.0+031519	bs	23 04 01.18 +03 15 18.5	early type spectrum	0.036	14.02 [1]	obs
XBSJ230434.1+122728	bs	23 04 34.25 +12 27 26.2	strong [OIII] and no Hβ	0.232	18.30 [1]	obs
XBSJ231546.5–590313	bs	23 15 46.76 –59 03 14.5	narrow emission lines	0.045	14.00 [2]	5

Column 1: name; Col. 2: sample (bs = [0.5–4.5 keV] BSS sample, hbs = [4.5–7.5 keV] HBSS sample); Col. 3: position of the optical counterpart; Col. 4: a short description of the optical spectrum; Col. 5: redshift; Col. 6: red magnitude: (1) = derived from APM E-magnitude; (2) red magnitude (either R or r) from the literature or computed from our own photometry; (3) = magnitude visually estimated from the DSS red plates; Col. 7: references to the spectrum.
obs = from our own spectroscopy;
[1] (SDSS J100032.24+553631.0) = spectrum from the SDSS (classified as galaxy). Also in RIXOS (Mason et al. 2000) and in Zhou et al. (2006) (Classified respectively as Sy 2 and NLSy1, see Appendix B for more details);
[2] (NGC 3607) = spectrum from Ho et al. (1995). Classified as LINER 2 in Ho et al. (1997);
[3] (NGC 4291) = spectrum from Ho et al. (1995);
[4] (RIXOS F223 097) = In Mason et al. (2000, the unpublished optical spectrum from RIXOS is reported in Fig. 2);
[5] (IRAS 23128-5919) = spectrum from Kweley et al. (2001). In the literature this object (an ULIRG) is classified as Sy2/Starburst.

~300 objects, including elliptical galaxies, groups and clusters of galaxies we have estimated the range of temperatures expected for a given X-ray luminosity and compared it with the best-fit one. All the sources for which a thermal model is acceptable have an X-ray luminosity below 6×10^{43} erg s^{-1} that corresponds to expected temperatures below 3 keV. In all these cases, instead, the best-fit temperatures range between 3 and 10 keV. These temperatures are usually observed only in very luminous clusters ($L_X = 10^{44}$–10^{46} erg s^{-1}). Even if we consider the uncertainties on the kT values, the lower limits on the temperatures are too high considering the observed X-ray luminosities in all cases.

In conclusion, a single thermal model, with physically acceptable temperatures, can be rejected confidently in all the objects.

In Table 2 we summarize the results of the X-ray analysis. The best-fit model is indicated in Col. 4. A value of temperature (Col. 7) reported between parenthesis means that a thermal model is, from a statistical point of view, alternative to the one indicated in Col. 4 but has been rejected as "unphysical" on the basis of the considerations discussed above.

3.1. X-ray evidence for AGN?

The presence of a power-law (or two power-laws) emission model in all the sources discussed here can be considered as suggestive for the presence of an AGN in all cases. It should be noted, however, that in the very low-luminosity regime ($L_X <$ a few 10^{40}) hard X-ray emission is often detected in elliptical

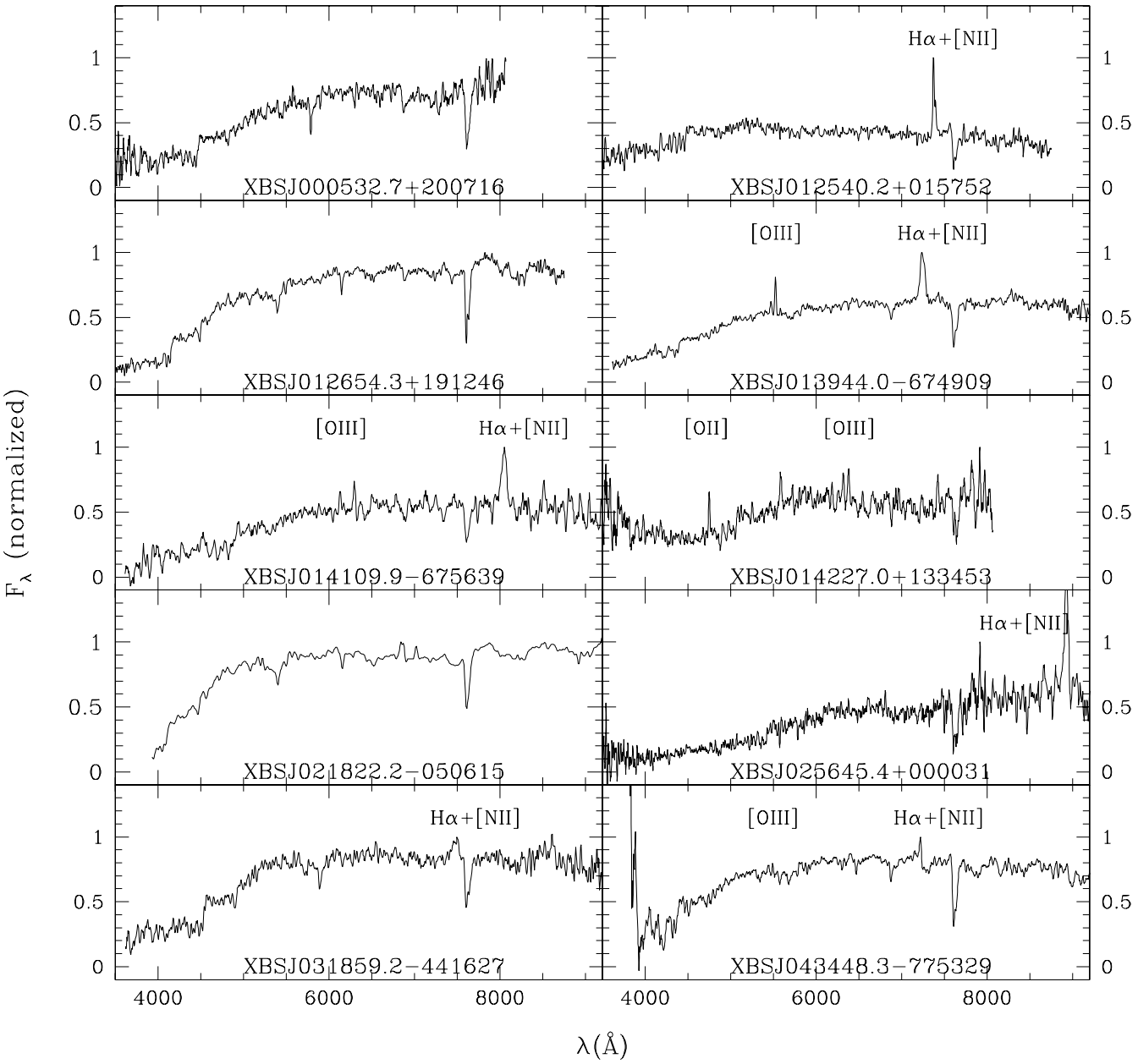

Fig. 2. The optical spectra of the elusive AGN candidates (we do not report the 4 spectra already published in the literature, see Table 1). The strongest emission lines are marked.

galaxies, besides the usual thermal emission associated with the hot gas ($kT \sim 1$ keV) (e.g. Matsushita et al. 1994). The origin of this emission has been attributed mainly to discrete binary X-ray sources (Matsushita et al. 1994). The confirmation that many ellipticals actually harbor a population of point-like sources with luminosities ranging from 10^{37} to 10^{39} erg s^{-1} or even (but rarely) above 10^{39} erg s^{-1}, has been produced by high resolution *Chandra* images (see Fabbiano & White 2006, for a review). The integrated X-ray luminosity of the X-ray binaries in elliptical and S0 galaxies typically ranges from 6×10^{39} to 9×10^{40} erg s^{-1} (Kim & Fabbiano 2004). For this reason, caution must be paid before considering the presence of a power-law fit as suggestive of the presence of an AGN in the low-luminosity regime ($<10^{41}$ erg s^{-1}). Only two objects in our sample, XBSJ111654.8+180304 (NGC 3607) and XBSJ122017.5+752217 (NGC 4291) have 2–10 keV luminosities below 10^{41} erg s^{-1}.

XBSJ111654.8+180304 (NGC 3607) is a LINER (Ho et al. 1997). The X-ray luminosity (1.1×10^{39} erg s^{-1}) is the lowest among the extragalactic XBS sources. The X-ray spectrum is well fitted by a steep power-law model ($\Gamma = 2.3$) plus a thermal component with $kT = 0.71$ keV. Based on Chandra (and HST) data, González-Martín et al. (2006) have concluded that the observed hard X-ray emission is extended and not related to a nuclear source.

XBSJ122017.5+752217 (NGC 4291) is a galaxy with an early-type spectrum with no emission lines. Its X-ray luminosity (2×10^{40} erg s^{-1}) is similar to those observed by Matsushita et al. (1994) and the X-ray spectral properties (a soft thermal component with $kT = 0.51$ keV plus a hard tail) could be either indicative of the presence of a very low-luminosity AGN or of the presence of a population of X-ray binaries. Observations in the soft X-ray with high spatial resolution, carried out by ROSAT High Resolution Imager (HRI), seem to

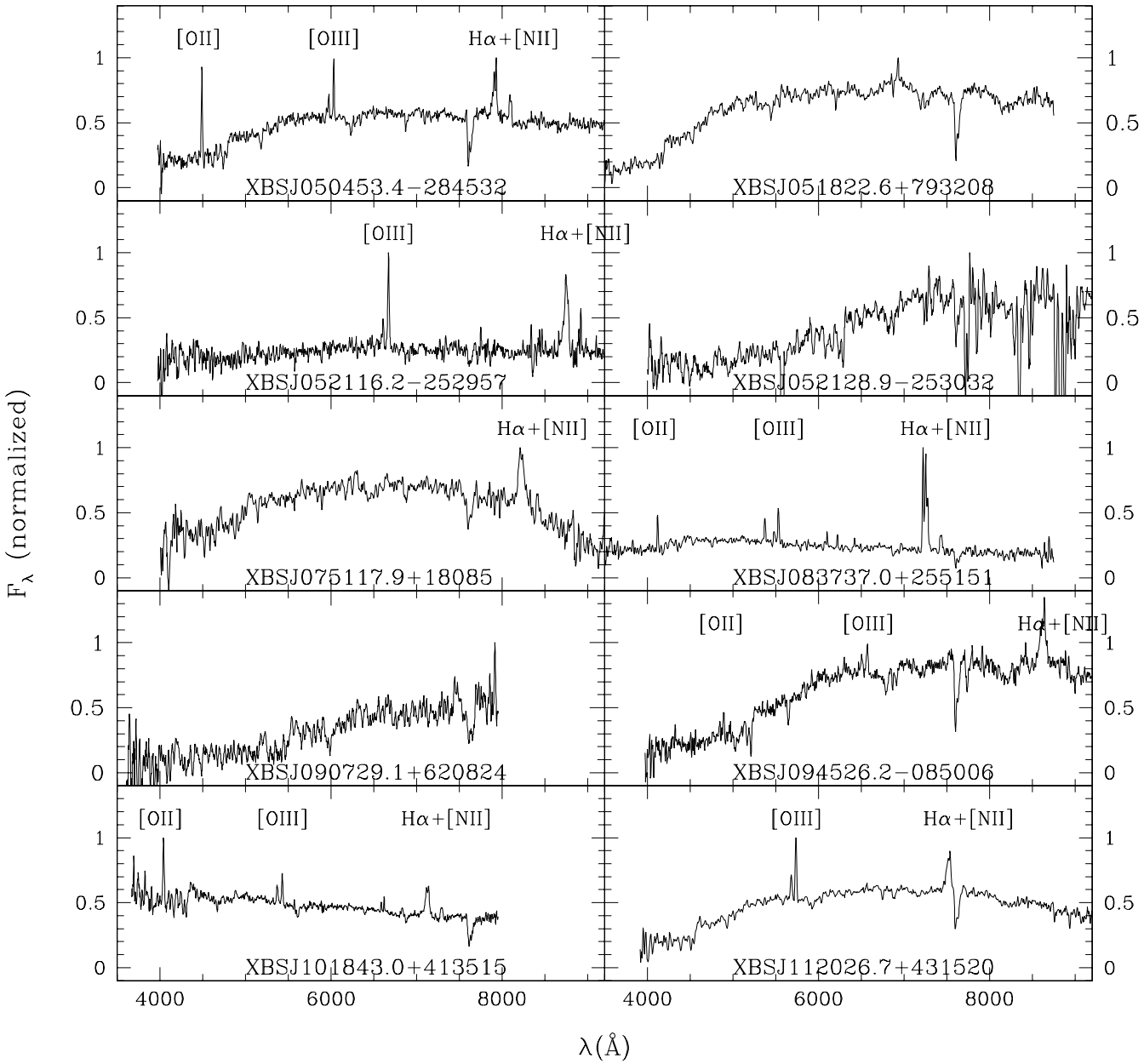

Fig. 2. continued.

favour the low-luminosity AGN hypothesis (Roberts & Warwick 2000; Liu & Bregman 2005) but the conclusion is uncertain. We tentatively classify this object as "non-AGN" and we do not consider it as AGN in the following analysis.

All the remaining sources have X-ray luminosities larger than 10^{41} erg s^{-1} and are well fitted only by a power-law model or a leaky model (in a few cases plus an additional thermal emission) and we consider these elements as strongly indicative of the presence of an AGN.

It must be noted that some of the 35 objects analysed here have an optical spectrum characterized by narrow emission lines suggestive of star-formation. Higher X-ray luminosities are expected in these cases when compared to "passive" elliptical galaxies. The most extreme cases are represented by the Ultraluminous Infrared Galaxies (ULIRG) where 2–10 keV luminosities[2] up to 2–3 × 10^{41} erg s^{-1} are often observed even if an AGN is not clearly present (e.g. Franceschini et al. 2003). All the objects in our sample with a starburst-like spectrum have 2–10 keV luminosities above 10^{42} erg s^{-1} and it is unlikely that it is all due to the starburst activity. For instance, the most extreme starburst in the sample (the ULIRG XBSJ231546.5-590313) has been studied in detail by Franceschini et al. (2003) and the AGN component has been clearly detected out of the starburst emission in the X-ray spectrum.

In conclusion, the X-ray spectral analysis has revealed in all but two sources the presence of an AGN which is either absorbed or unabsorbed/mildly absorbed. This result confirms what has been already estimated from the X-ray-to-optical flux ratios and the observed X-ray luminosities i.e. that most of the 35 objects discussed here actually contain an AGN.

Given the impossibility of using the optical spectra for a reliable classification of the elusive AGN we have decided to use the results of the X-ray analysis to classify these objects. In order to match the optical classification into type 1 and type 2 AGN

[2] Converted into the cosmology adopted here.

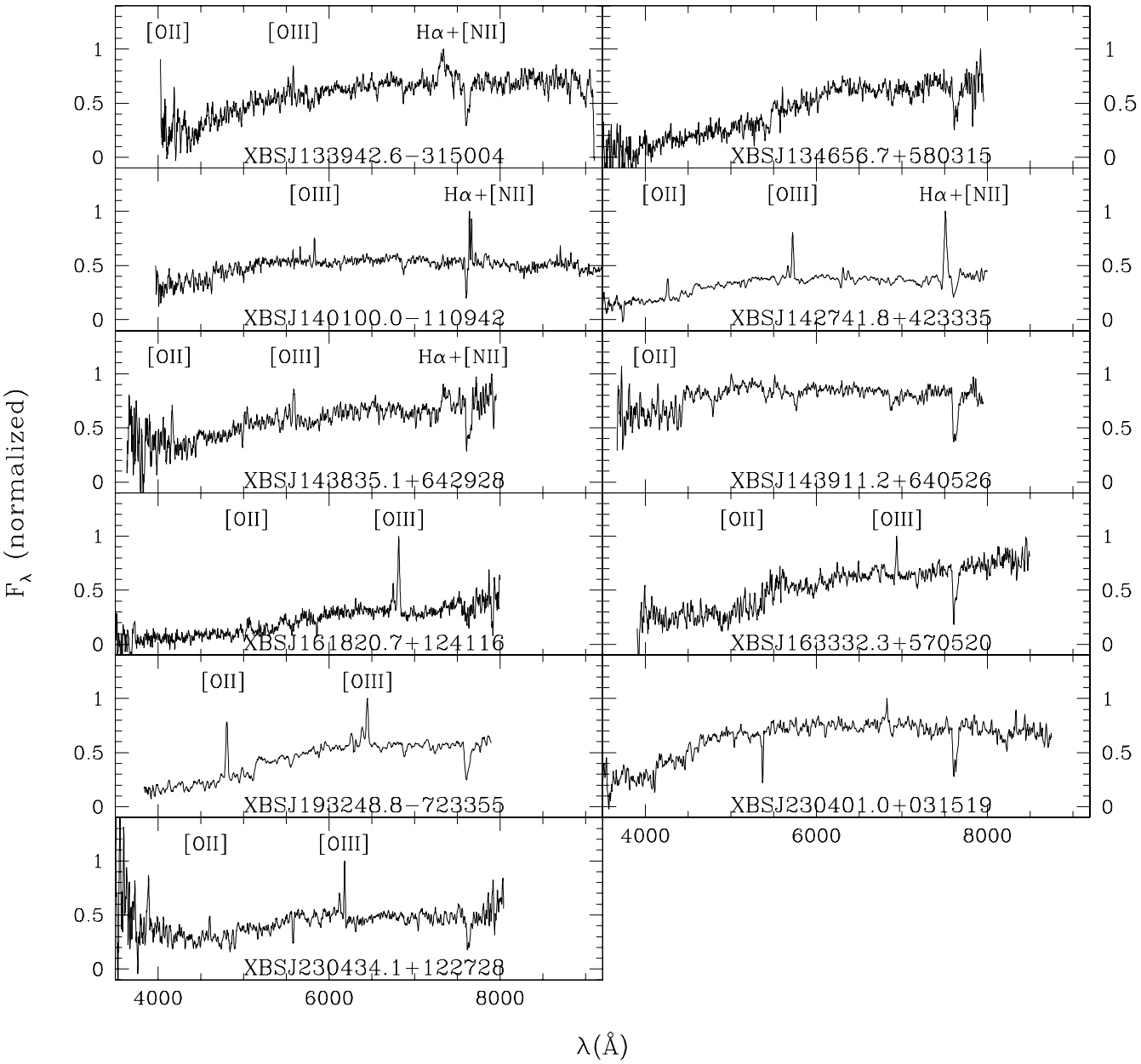

Fig. 2. continued.

adopted for the XBS sources, that corresponds to a dividing limit on the optical absorption of A_V of ∼2 mag, as discussed in Caccianiga et al. (2007, in prep.), we have used the corresponding value of $N_{\rm H} = 4 \times 10^{21}$ cm^{-2} (assuming the Galactic standard $N_{\rm H}/A_V$ relation) to separate the elusive AGNs into type 1 and type 2. With this threshold we thus classify 11 objects as "type 2" AGN and 20 objects as type 1 AGN. We have considered as non-absorbed also an object (XBSJ000532.7+200716) for which we have determined an upper limit on $N_{\rm H}$ which is marginally higher than 4×10^{21} cm^{-2}. Finally, for one source (XBSJ012654.3+191246) the upper limit on $N_{\rm H}$ is not stringent enough ($<1.2 \times 10^{22}$ cm^{-2}) to allow a classification of the source.

4. Why are they hidden in the optical?

The X-ray analysis discussed in the previous section has demonstrated the presence of an AGN in all but two sources studied here. We now want to investigate the reason (or the reasons) why the AGN is hardly detected (or not detected at all) in the optical band.

Different hypothesis have been discussed in the recent literature to explain the presence of a large number of "optically dull" sources in X-ray surveys. Comastri et al. (2002, 2003), for instance, have suggested that an heavily absorbed AGN (Compton thick with $N_{\rm H} > 10^{24}$ cm^{-2}) could be hidden within some XBONG. This hypothesis is suggested by the fact that, in the magnitude/X-ray flux plot, the XBONG discovered in *Hellas2XMM* survey occupy a region where also Compton thick AGN are expected to be found, given their typical spectral energy distribution and redshift (Comastri et al. 2003). Alternatively, it has been proposed by different authors (Moran et al. 2002; Severgnini et al. 2003; Georgantopoulos & Georgakakis 2005; Page et al. 2006) that the elusiveness of many X-ray selected AGN is just the consequence of the intrinsic weakness (in respect to the host-galaxy) combined in

Table 2. X-ray spectroscopy.

Name	z	Net counts	Model	Γ	$N_{\rm H}$	kT	Red. χ^2 /d.o.f.	Log $L_{\rm X}$	X-ray class
					[10^{22} cm^{-2}]	[keV]		[erg s^{-1}]	
XBSJ000532.7+200716	0.11900	1118	BB+PL	$2.32^{+0.52}_{-0.30}$	<0.49	0.10	0.98 / 39	42.39	nabs AGN
XBSJ012540.2+015752	0.12310	697	PL	$1.79^{+0.15}_{-0.12}$	<0.03	...	1.35 / 37	42.62	nabs AGN
XBSJ012654.3+191246	0.04268	154	T+PL	$1.95^{+0.71}_{-0.39}$	<1.20	0.99	1.14 / 5	41.25	AGN
XBSJ013944.0−674909	0.10400	794	PL	$1.94^{+0.14}_{-0.12}$	<0.02	...	0.91 / 34	42.56	nabs AGN
XBSJ014109.9−675639	0.22600	408	PL	$1.78^{+0.39}_{-0.34}$	$0.12^{+0.21}_{-0.12}$	(5.80)	0.72 / 16	43.53	nabs AGN
XBSJ014227.0+133453	0.27500	120	PL	$1.80^{+0.72}_{-0.53}$	$0.15^{+0.38}_{-0.15}$	(8.80)	0.70 / 3	43.44	nabs AGN
XBSJ021822.2−050615[1]	0.04400	1772	Leaky+Line	$1.66^{+0.34}_{-0.36}$	$20.54^{+0.36}_{-0.44}$	...	1.41 / 63	42.53	abs AGN
XBSJ025645.4+000031	0.35850	399	PL	$1.93^{+0.37}_{-0.19}$	<0.14	(4.10)	1.15 / 15	43.48	nabs AGN
XBSJ031859.2−441627[1]	0.13954	350	PL	$1.72^{+0.43}_{-0.37}$	$0.39^{+0.34}_{-0.28}$	...	0.80 / 14	42.99	nabs AGN
XBSJ043448.3−775329	0.09700	244	PL	$1.50^{+0.12}_{-0.11}$	$0.27^{+0.12}_{-0.11}$	...	1.23 / 33	42.86	nabs AGN
XBSJ050453.4−284532	0.20400	1205	PL	$1.45^{+0.12}_{-0.14}$	$0.04^{+0.04}_{-0.04}$	...	0.86 / 54	43.16	nabs AGN
XBSJ051822.6+793208	0.05250	979	PL	$1.86^{+0.11}_{-0.11}$	<0.02	...	0.90 / 43	41.83	nabs AGN
XBSJ052116.2−252957	0.33200	151	PL	$2.10^{+0.75}_{-0.34}$	<0.32	(3.30)	0.74 / 6	43.22	nabs AGN
XBSJ052128.9−253032	0.58750	60	PL	1.9 (frozen)	$12.71^{+6.46}_{-3.98}$	...	0.87 / 5	44.45	abs AGN
XBSJ075117.9+180856[1]	0.25500	913	PL	$1.58^{+0.16}_{-0.16}$	$0.11^{+0.07}_{-0.07}$	...	0.86 / 42	43.50	nabs AGN
XBSJ083737.0+255151	0.10520	261	PL	$1.77^{+0.35}_{-0.33}$	$0.34^{+0.30}_{-0.22}$	...	0.75 / 14	43.00	nabs AGN
XBSJ090729.1+620824	0.38800	90	PL	1.9 (frozen)	$0.90^{+1.58}_{-0.62}$	...	1.90 / 3	43.63	abs AGN
XBSJ094526.2−085006	0.31400	136	PL	$2.22^{+1.24}_{-0.75}$	$0.32^{+0.87}_{-0.32}$	(5.90)	1.66 / 5	43.49	nabs AGN
XBSJ100032.5+553626	0.21600	266	Leaky	$2.26^{+0.42}_{-0.29}$	$25.70^{+84.60}_{-21.10}$	...	0.86 / 13	43.93	abs AGN
XBSJ101843.0+413515	0.08400	837	PL	$1.87^{+0.18}_{-0.11}$	<0.04	...	1.11 / 41	42.30	nabs AGN
XBSJ111654.8+180304	0.00312	822	T+PL	$2.25^{+0.37}_{-0.25}$	<0.07	0.71	0.66 / 34	39.00	GAL
XBSJ112026.7+431520	0.14600	412	Leaky+Line	$1.65^{+0.83}_{-0.42}$	$6.28^{+3.21}_{-1.73}$	...	0.88 / 21	43.20	abs AGN
XBSJ122017.5+752217	0.00586	8190	T+PL	$2.35^{+0.55}_{-0.45}$	$1.45^{+0.81}_{-0.63}$	0.51	0.99 / 231	40.20	GAL?
XBSJ133942.6−315004	0.11409	1076	PL	$1.62^{+0.22}_{-0.18}$	$0.23^{+0.12}_{-0.08}$	...	1.32 / 50	42.81	nabs AGN
XBSJ134656.7+580315	0.37300	106	PL	1.9 (frozen)	$9.50^{+4.72}_{-3.16}$	...	1.92 / 13	44.04	abs AGN
XBSJ140100.0−110942	0.16400	1305	PL	$2.33^{+0.11}_{-0.10}$	<0.02	...	1.23 / 57	42.57	nabs AGN
XBSJ142741.8+423335	0.14200	487	PL	1.9 (frozen)	$4.48^{+0.93}_{-0.77}$	...	0.85 / 23	43.20	abs AGN
XBSJ143835.1+642928	0.11800	404	PL	$1.84^{+0.42}_{-0.18}$	$1.85^{+0.73}_{-0.55}$	...	0.73 / 23	43.03	abs AGN
XBSJ143911.2+640526	0.11290	123	PL	1.9 (frozen)	$20.00^{+9.72}_{-6.56}$	...	0.52 / 6	42.96	abs AGN
XBSJ161820.7+124116	0.36100	40	PL	1.9 (frozen)	$4.96^{+6.14}_{-2.48}$	...	1.17 / 3	43.72	abs AGN
XBSJ163332.3+570520	0.38600	613	PL	$2.19^{+0.72}_{-0.39}$	$0.03^{+0.29}_{-0.03}$	(3.70)	0.78 / 16	43.45	nabs AGN
XBSJ193248.8−723355	0.28700	782	PL	$1.48^{+0.25}_{-0.22}$	$0.73^{+0.35}_{-0.29}$	...	0.86 / 33	43.80	abs AGN
XBSJ230401.0+031519	0.03630	183	PL	$1.78^{+0.88}_{-0.24}$	<0.15	(4.30)	0.95 / 5	41.47	nabs AGN
XBSJ230434.1+122728	0.23200	180	PL	$1.52^{+0.43}_{-0.37}$	<0.18	...	1.08 / 5	43.31	nabs AGN
XBSJ231546.5−590313[2]	0.04460	833	T+Leaky	$1.67^{+0.09}_{-0.34}$	$6.90^{+4.70}_{-3.40}$	0.65	0.74 / 44	42.04	abs AGN

Column 1: name ([1] = X-ray analysis taken from Severgnini et al. 2003; [2] = X-ray analysis taken from Franceschini et al. 2003); Col. 2: redshift; Col. 3: net counts used for the spectral analysis; Col. 4: best-fit model (PL = single absorbed power-law model; BB = black-body emission; T = Thermal (Mekal) model; Leaky = Leaky model (see text for details); Col. 5: power-law photon index; Col. 6: intrinsic absorption column density; Col. 7: best-fit temperature of the additional thermal component or, if in parenthesis, the temperature of the thermal model (alternative to the power-law model, see text for details); Col. 8: reduced χ^2 and degrees of freedom of the best-fit model; Col. 9: Log of the de-absorbed 2–10 keV X-ray luminosity; Col. 10: classification based on the X-ray analysis: nabs AGN = non-absorbed (or partly absorbed) AGN ($N_{\rm H} < 4 \times 10^{21}$ cm^{-2}); abs AGN = absorbed AGN ($N_{\rm H} > 4 \times 10^{21}$ cm^{-2}); GAL = X-ray from normal galaxy (thermal and/or from X-ray binaries).

some cases with moderate absorption (10^{22} cm^{-2}–10^{24} cm^{-2}) of an otherwise "normal" AGN. This effect, often called "optical dilution", is expected when the optical spectra are taken with a relatively large slit width including a large amount of star-light from the host-galaxy. Another possible explanation is that the "optically-dull" AGN (or at least a fraction of them) are characterized by unusual properties like a weak emission from the accretion disk (e.g. a radiatively inefficient accretion flow RIAF, Yuan & Narayan 2004) that produces extremely "flat" values of $\alpha_{\rm OX}$[3] spectral index. Similarly, a BL Lac object can be a valid possibility (Brusa et al. 2003) although, given the low space density of these objects, it is unlikely that this explanation can account for all (or a large fraction) of the "elusive" AGN selected in a X-ray survey. Finally, the entire AGN (including the Narrow Line Region) could suffer from extra-torus absorption, located, for instance, on large scales within the host galaxy (e.g. Rigby et al. 2006; Cocchia et al. 2007). Rigby et al. (2006), in particular, consider that, at high-redshifts (>1) besides the host-galaxy dilution the extra-nuclear dust in the host galaxy is likely to contribute to hide the AGN.

[3] The two point spectral index $\alpha_{\rm OX}$ is defined as: $\alpha_{\rm OX} = -\frac{\rm Log(f_o/f_x)}{\rm Log(\nu_o/\nu_x)}$ where f_o and f_x are, respectively, the monochromatic fluxes at $\nu_o = 1.20 \times 10^{15}$ Hz (corresponding to $\lambda_o = 2500$ Å) and $\nu_x = 4.84 \times 10^{17}$ Hz (corresponding to $E = 2$ keV).

In the following sections we analyse all these competing hypotheses to assess their relative importance to explain the "elusive AGN" found in the XBS survey.

4.1. Compton-thick hypothesis

The detection of a Compton-thick AGN, using the 2–10 keV energy band may be missed, in particular for local AGN, since the energy cut-off is expected to fall outside the observed interval. Other indicators can be used to assess its presence, like the detection of a prominent Fe Kα emission line at 6.4 keV or a very low (<1) $F_X/F_{[OIII]}$ flux ratio. This latter indicator, called Compton-thickness parameter (T), is relatively easy to apply and its reliability has been already tested (Bassani et al. 1999) at least for local AGN. The indicator is based to the fact that, in presence of a high level of absorption, the 2–10 keV flux is expected to be heavily suppressed while the [OIII]λ5007 Å should be unaffected. The available X-ray spectra of the elusive XBS AGNs do not have – on average – enough counts to asses the presence of the Kα line or to compute a stringent upper limit. For this reason we use the T parameter to test the Compton-thick hypothesis.

The optical spectra of the XBS sources have been taken with the primary aim of deriving the spectral classification and the redshift. Since both quantities do not require a reliable absolute calibration, the observing runs are not necessarily carried out under photometric conditions and no corrections have been applied, for instance, for the flux-loss due to the width of the slit. Using the magnitudes available for the XBS objects we have statistically corrected the fluxes in each observing run and estimated the uncertainty on the final flux which turned out to have a relative error of ∼50% (see Appendix A for details).

In Fig. 3 we report the Compton-thickness parameter as a function of the X-ray flux for all the 35 objects discussed in this paper i.e. including the 2 sources classified as normal galaxies. We have corrected the [OIII]λ5007 Å fluxes for the extinction due to our Galaxy. The extinction due to the host galaxy is more difficult to estimate given the type of spectra under analysis (e.g. the Balmer decrement cannot be measured). However we can evaluate the maximum level of extinction that can be expected given the type of galaxies under analysis. The largest levels of extinction are expected for galaxies with high star-forming where extinctions up to $A_V \sim 1$ can be observed (Calzetti & Heckman 1999). In the majority of the elusive AGN discussed here, however, the host-galaxy does not show evidence of high star-formation rate given the absence (or the weakness) of emission lines and, therefore, the extinction is expected to be well below 1 mag. Only for the few emission lines galaxies in the sample the extinction could reach $A_V \sim 1$ (the most extreme case is XBSJ231546.5-590313, an ULIRG whose optical spectrum is dominated by the star-formation). The maximum variation of the Compton-thickness parameter expected in these cases is reported in the box located in the upper-left side of Fig. 3.

From Fig. 3 it is clear that all the elusive sources in the XBS survey have a Compton-thickness parameter well above 1. Considering the maximum level of extinction (∼1 mag) due to the host-galaxy only the three objects with $T < 10$ fall close (but not within) the Compton-thick region. Two of these sources are tentatively classified as "normal" galaxies (XBSJ111654.8+180304 and XBSJ122017.5+752217, see discussion in Sect. 3.1) although in one of these (XBSJ122017.5+752217) the actual absence/presence of an AGN is still debated. The third source (XBSJ012654.3+191246) has been classified as AGN on the basis of the X-ray emission

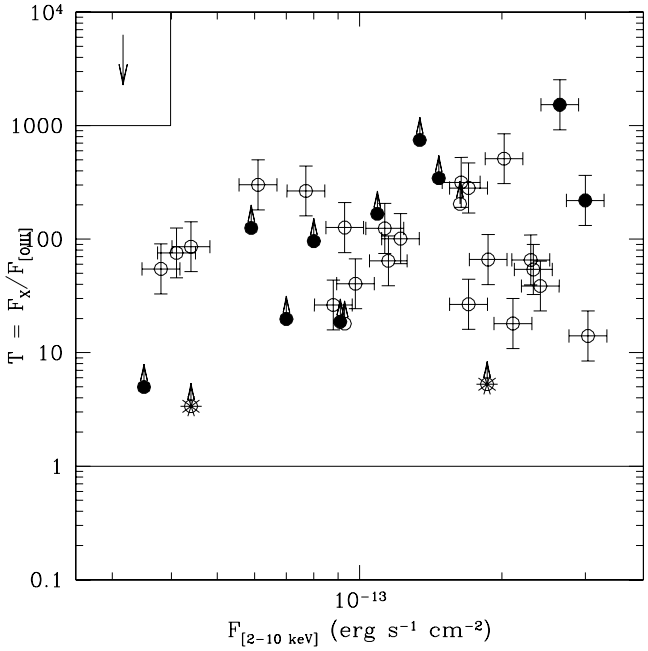

Fig. 3. The Compton-thickness parameter (corrected for Galaxy extinction) versus the X-ray flux of the elusive AGN and normal galaxies of the XBS sources. Circles represent the sources classified as AGN from the X-ray analysis. Filled circles, in particular, are the sources with an early-type spectrum (XBONG). The two stars are the sources that probably do not contain an AGN (see text for details). The arrow within the box in the upper-left side of the figure represents the maximum variation of T due to the host-galaxy extinction.

but its further characterization as absorbed or unabsorbed is not possible given the high upper limit on the intrinsic value of N_H. The 2–10 keV luminosities of these three sources are the lowest observed in the XBS survey (between 10^{39} and 2×10^{41} erg s^{-1}). At present we can rule out the Compton-thick hypothesis for XBSJ111654.8+180304 for which high-resolution X-ray data (Chandra) have not detected any hard point-like nucleus in this object (González-Martín et al. 2006). For the remaining two sources we need additional data (e.g. high S/N X-ray spectrum to detect or rule out the presence of the Fe Kα emission line).

We conclude that the Compton-thick hypothesis is not supported for most (if not all) of the elusive AGN in the XBS survey. Indeed, the presence of a Compton thick AGN should produce strong narrow emission lines in the optical spectrum of sources with bright X-ray fluxes (>10^{-13} erg s^{-1} cm^{-2}) something that, by definition, is not found among the elusive objects.

4.2. Weakness/moderate absorption

In Fig. 4 we report the 4000 Å break (Δ[4]) versus the unabsorbed X-ray luminosities of all the XBS objects. The 4000 Å break is a rough indicator of the importance of the galaxy star-light in the total emission of the source. When the nuclear emission is dominant (at ∼4000 Å, source's rest-frame), the value of Δ is just an indicator of the slope of the nuclear emission: the bluer the spectrum, the lower (typically negative) the value of Δ. In

[4] The 4000 Å break is defined as $\Delta = \frac{F^+ - F^-}{F^+}$ where F^+ and F^- represent the mean value of the flux density (expressed per unit frequency) in the region 4050–4250 Å and 3750–3950 Å (in the source's rest-frame) respectively.

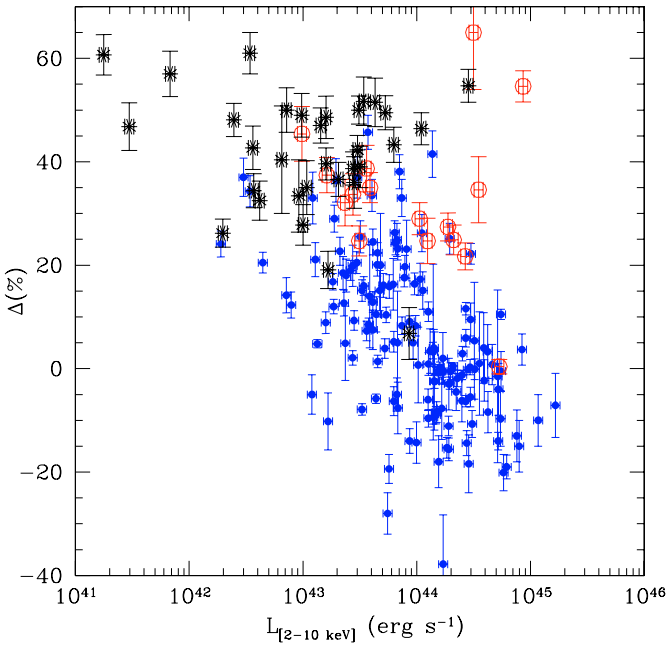

Fig. 4. The 4000 Å break (Δ), given in percentage, versus the de-absorbed 2–10 keV X-ray luminosity for the XBS sources. Filled points are type 1 AGN, open circles are type 2 AGN, stars are elusive AGN.

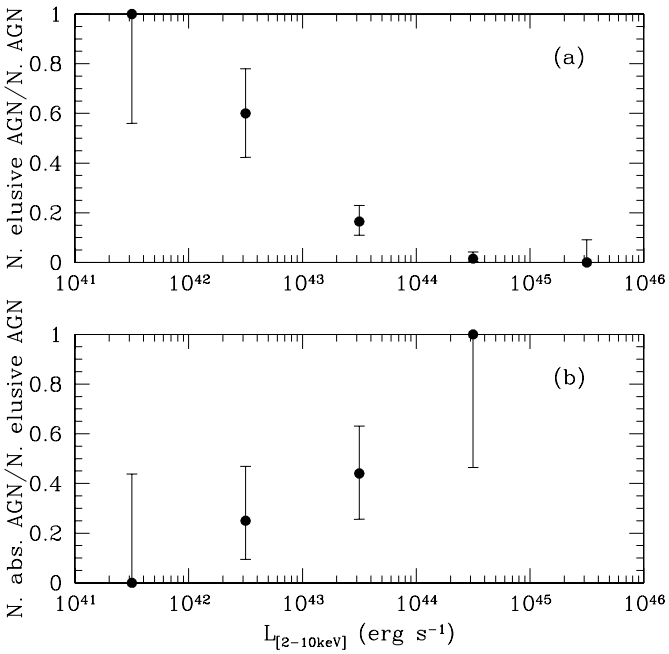

Fig. 5. a) Fraction of elusive AGN as a function of the 2–10 keV de-absorbed X-ray luminosity; **b)** Fraction of absorbed AGN among the elusive AGN. The error-bars are computed using a Bayesian method: in particular, we plot the shortest 90% confidence interval.

these cases the value of Δ is usually below 20%. When, on the contrary, the continuum is dominated by the host galaxy light the value of Δ ranges from 20% up to 60%, depending on the type of host-galaxy. In the 20%–40% range of Δ we find also sources where both the nucleus and the host galaxy contribute to the observed spectrum.

The X-ray luminosity is an independent indicator of the AGN strength, at least in the 33 sources for which the presence of an AGN has been assessed (the 2 "normal" galaxies are not plotted in this figure).

Figure 4 shows an evident anti-correlation between Δ and the X-ray luminosity: powerful ($L_X > 10^{44}$ erg s^{-1}) AGN are only marginally affected by the recognition problem, and the host-galaxy contribution to the total emission at 4000 Å is usually low or negligible (Δ < 30%); for X-ray luminosities between 10^{43} and 10^{44} erg s^{-1} the fraction of elusive AGNs becomes more important and the values of Δ range from −30 to 50%; in the low-luminosity regime (<10^{43} erg s^{-1}) the majority of the sources is optically elusive and Δ is in the typical range of values observed in galaxies (20%–60%). This trend is shown in Fig. 5a which reports the fraction of elusive AGN as a function of the de-absorbed 2–10 keV X-ray luminosity.

The observed trend is a first indication supporting the hypothesis that optically elusive AGN are simply the low-luminosity tail of the AGN population.

In Fig. 5b the fraction of elusive AGN classified as "absorbed" AGN ($N_H > 4 \times 10^{21}$ cm^{-2}) according to the X-ray analysis has been reported. For X-ray luminosities below 10^{43} erg s^{-1} the fraction of absorbed AGN among the elusive AGN is similar to the fraction of absorbed AGN among the total sample of AGN in the XBS survey (∼10%–30% in the BSS and HBSS samples respectively). For higher X-ray luminosities, instead, the fraction of absorbed objects among elusive AGN increases significantly and becomes dominant for luminosities >10^{44} erg s^{-1}. The obvious interpretation of this trend is that, beside the luminosity of the AGN, also the absorption (but still in Compton-thin regime) plays an important role to "hide" the AGN and, for high X-ray luminosities (>10^{44} erg s^{-1}), this becomes the most important explanation.

In Fig. 6 we show the values of 4000 Å break versus the [OIII]λ5007 Å equivalent widths for the type 1, type 2 and the optically elusive AGN in the XBS survey. The [OIII]λ5007 Å emission line is a good indicator of the AGN activity, being unaffected by the absorption (according to the simplest version of the unified models). On the same figure we plot the expected "paths" (continuous lines) of a source that is absorbed from 0 up to $A_V \sim 500$ (corresponding to $N_H \sim 10^{24}$ assuming the Galactic standard A_V/N_H conversion). To produce these curves we have used the spectral model discussed in Severgnini et al. (2003). This model includes a galaxy and an AGN template. The AGN template, in particular, is composed by two parts: a) the continuum with the broad emission lines and b) the narrow emission lines. According to the basic version of the AGN unified model, the first part can be absorbed while the second one is not affected by the presence of an obscuring medium. The AGN template is based on the data taken from Francis et al. (1991) and Elvis et al. (1994) while the extinction curve is taken from Cardelli et al. (1989). The galaxy template is produced on the basis of the Bruzual & Charlot (2003) models.

In Fig. 6 we have considered 3 examples of curves where the intrinsic (i.e. not absorbed) AGN/galaxy flux ratio at 4050 Å ($\eta_{4050\ Å}$[5]) is, respectively, ∼60, 3 and 0.4. On the same plot we show the region corresponding to an absorption of $A_V = 2$ mag (dashed line). To produce these curves we have assumed an host galaxy of $t = 10$ Gyr. To show the impact of this assumption on the plotted curves we report on the same figure also the $A_V = 2$ mag line computed assuming a much younger host galaxy ($t = 1$ Gyr instead of 10 Gyr, dotted line).

[5] We define $\eta_{4050\ Å} = \frac{f_{AGN}(4050\ Å)}{f_{Gal}(4050\ Å)}$ where $f_{AGN}(4050$ Å) and $f_G(4050$ Å) are the monochromatic fluxes at 4050 Å (source's rest-frame) that pass through the slit of the spectrograph.

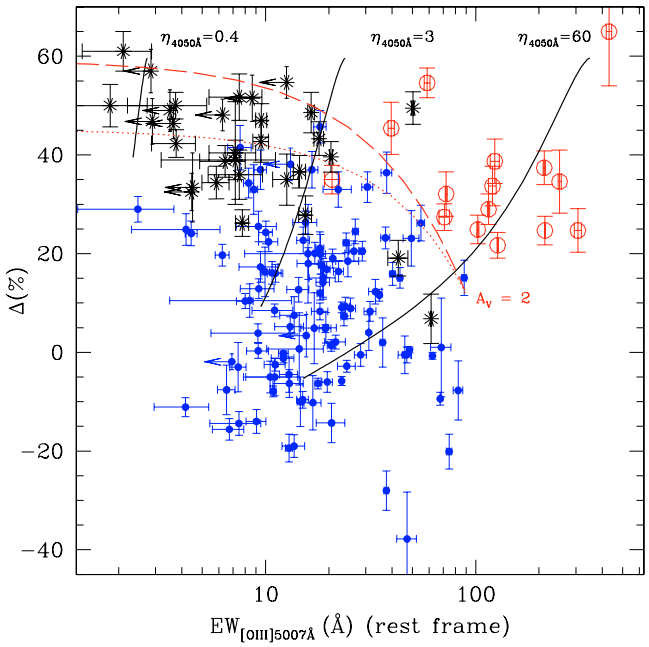

Fig. 6. The 4000 Å break (Δ), given in percentage, versus the [OIII]λ5007 Å equivalent width of the type 1 AGN (filled points), type 2 AGN (open circles) and the optically elusive AGN (stars). The 3 solid lines labeled as $\eta_{4050\ Å} = 0.4$, 3 and 60 show the expected "paths" followed when the optical absorption increases from 0 to $A_V \sim 500$ in sources with an intrinsic AGN/host-galaxy flux ratio ($\eta_{4050\ Å}$) of 0.4, 3 and 60 respectively. The dashed line shows the region corresponding to an absorption level of $A_V = 2$ mag. The dotted line shows how the $A_V = 2$ mag line changes when a younger host galaxy is assumed ($t = 1$ Gyr instead of 10 Gyr).

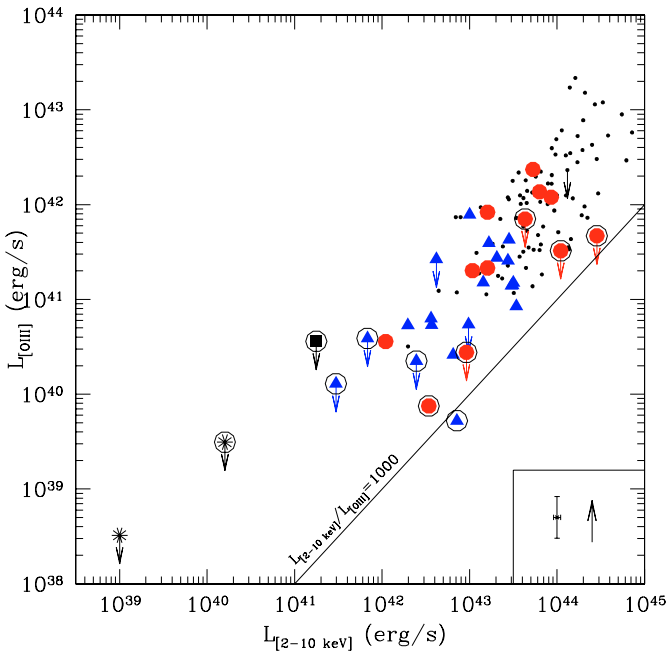

Fig. 7. The [OIII]λ5007 Å luminosity versus the de-absorbed 2–10 keV X-ray luminosity for the type 1 AGN of the XBS survey (small points), the elusive AGN (filled points = type 2 AGN, filled triangles = type 1 AGN, filled box = AGN without further characterization into type 1 or type 2) and the 2 normal galaxies (stars). The arrows correspond to the sources where the [OIII] emission line is not detected. The sources with an early-type spectrum (i.e. XBONG-like) are circled. The continuous line is the limit proposed by Cocchia et al. (2007) to classify an object as XBONG. For clarity, we have reported the typical error-bar in the right-bottom box. The arrow within this box indicates the expected maximum correction for extinction due to the host-galaxy (see discussion in Sect. 4.1 for details).

Figure 6 confirms and quantifies what has been already suggested by Fig. 4: when the AGN is intrinsically powerful, if compared to the host galaxy (e.g. $\eta_{4050\ Å} > 3$), optically absorbed and unabsorbed AGNs can be clearly detected and separated on the basis of the usual spectral classification criteria (see Caccianiga et al. 2007, in prep.) in the large majority of cases (∼95%). When the AGN is optically weak compared to the host galaxy ($\eta_{4050\ Å} < 3$) the optical classification becomes difficult or impossible in ∼55% of the cases. This percentage reaches ∼100% when the absorption level is high ($A_V > 2$).

The discussion presented above supports the idea that the intrinsic weakness of the AGN is the major reason for the optical dullness of the observed spectrum, at least for X-ray luminosities below 10^{43} erg s^{-1}. The presence of absorption ($N_H < 10^{22}$ cm^{-2}) is an additional element that further reduces the probability of detecting the AGN in the optical spectrum making the problem of dilution more important for type 2 AGN (∼40% are elusive) in respect to type 1 AGN (8% are elusive). For X-ray luminosities higher than 10^{44} erg s^{-1}, instead, the absorption is the most important reason for the AGN elusiveness. The result that "optical dilution", besides the absorption, is an important ingredient for the lack of broad emission lines in many low-luminosity ($L_X < 10^{43}$ erg s^{-1}) AGNs has been recently suggested by Page et al. (2006), thus indicating that this result holds also at fainter (10^{-15}–5×10^{-14} erg s^{-1} cm^{-2}) X-ray fluxes.

4.3. *Intrinsically flat α_{OX} or host-galaxy absorption hypothesis*

We want to test here whether the XBS elusive sources (or a fraction of them) show a particularly "flat" value of α_{OX} (<1) or unusual luminosities of the Narrow-Line Region (when compared to the X-ray luminosity). To this end, we first compute the luminosity of the [OIII]λ5007 Å emission line which is generally considered as a good tracer of the intrinsic AGN power.

In Fig. 7 the [OIII]λ5007 Å luminosity is plotted against the de-absorbed X-ray luminosity. We plot both the non-elusive type 1 AGN of the XBS survey and the elusive AGN. The [OIII] luminosities are corrected only for the Galactic extinction. The objects with a "passive" optical spectrum (i.e. the XBONG-like) are marked with a circle. On the same plot we report the line corresponding to $L_{[2-10\ keV]}/L_{[OIII]} = 1000$ that has been recently proposed to classify more properly the XBONG and to separate them from the rest of the AGN (Cocchia et al. 2007).

Figure 7 shows the (expected) correlation between the two luminosities but it does not reveal a different behaviour of the elusive AGN in respect to "confirmed" type 1 AGN: In the low-luminosity regime ($L_X < 10^{43}$ erg s^{-1}) the expected luminosity of the [OIII]]λ5007 Å emission line is simply too low to be detected out from the host-galaxy light.

This result is even more evident by plotting the distribution of the $L_{[2-10\ keV]}/L_{[OIII]}$ ratios for the type 1 AGN and the elusive AGN (Fig. 8). The majority of the elusive AGN have $L_{[2-10\ keV]}/L_{[OIII]}$ ratios well within the distribution

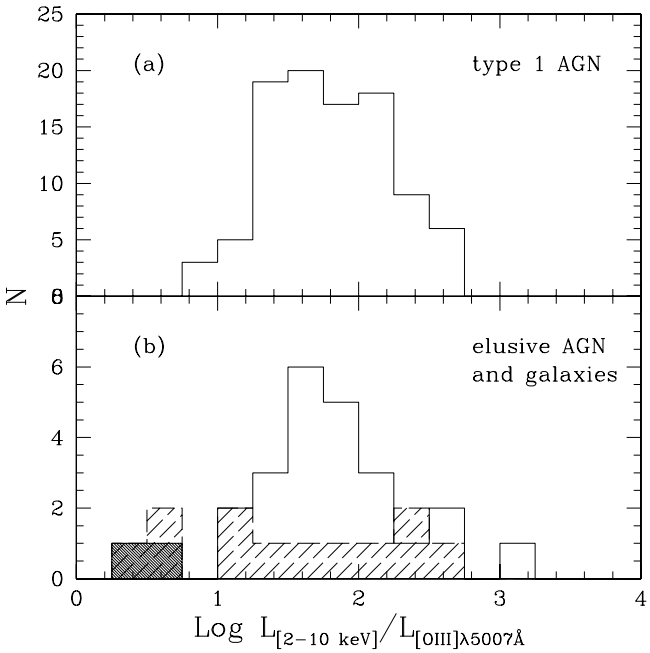

Fig. 8. The distribution of the 2–10 keV/[OIII]λ5007 Å luminosity ratio for the type 1 AGN (panel **a)**) and the elusive AGN plus normal galaxies (panel **b)**). Shaded histogram represent the lower limits for the sources where the [OIII] emission line is not detected. The two sources classified as normal galaxies are marked with an heavier shadowing.

observed in the type 1 AGN. In the XBS survey we have only one object (XBSJ043448.3−775329) which is located in the region below the $L_{[2-10\ \mathrm{keV}]}/L_{[\mathrm{OIII}]} = 1000$ line plus one additional source (XBSJ052128.9−253032) whose upper limit on the [OIII]λ5007 Å luminosity is just above this line.

We have analysed in more detail these 2 objects. Starting from the results of the X-ray analysis (L_X and N_H) we have applied the spectral model as discussed in Severgnini et al. (2003) to constrain the value of the nuclear α_{OX}. In summary, given the X-ray luminosity and an assumption on the value of α_{OX} we compute the intrinsic optical luminosity of the nucleus (before the absorption) and consequently normalize the AGN template. We then absorb the continuum and the broad lines of the template according to the value of N_H found from the X-ray data and sum the result to the host-galaxy template. The normalization of the galaxy template is fixed by reproducing the continuum of the observed optical spectrum. The nuclear α_{OX} is then estimated as the value that best reproduces the observed spectrum. In the case of the 2 objects discussed here the values of α_{OX} inferred from this analysis are $\leq$1.1, for XBSJ052128.9−253032 while we find $\alpha_{OX} \sim 1.1$ for XBSJ043448.3−775329. The two values are extreme but still within the distribution of α_{OX} values observed in type 1 AGN in the XBS survey (that have α_{OX} between 1 and 1.8, with a mean value of $\alpha_{OX} \sim 1.35$).

In conclusion, there are no strong indications that the elusive AGNs selected in the XBS survey have values of α_{OX} or of $L_{[OIII]}/L_X$ ratio significantly different from those observed in the entire AGN population selected in the survey once the intrinsic spread on the α_{OX} or the $L_{[OIII]}/L_X$ ratio is considered.

4.4. BL Lac objects

At least one elusive AGN, selected in the *Hellas2XMM* survey, has been classified as a possible BL Lac nucleus (Brusa et al. 2003). Indeed, the recognition problem is particularly critical for BL Lac objects due to their characteristic featureless continuum (Browne & Marcha 1993) and the fraction of mis-classified BL Lacs in medium/deep X-ray survey could be significant (Marchã & Browne 1995). However, given the relative low space density of this kind of AGN it is unlikely that the BL Lac hypothesis can account for more than "a few" elusive AGN. Indeed, on the basis of the X-ray $\log N - \mathrm{Log}S$ of BL Lacs derived from the *EMSS* survey (Wolter et al. 1991), at the flux limit of the XBS survey we expect about 2–7 BL Lac objects in total, a range which is consistent with the number of BL Lac (or candidates) already detected in the survey (5, Caccianiga et al. 2007, in prep.). Therefore, we do not expect that many (1–2 at most) BL Lac have been mis-classified in the XBS survey and included among the "elusive AGN".

Since BL Lac objects are radio emitters, it is possible to use the radio detection as a method to find out the mis-classified BL Lacs out of the 33 elusive AGN in the XBS survey. No dedicated radio follow-up has been scheduled for the XBS objects. However we can use the existing radio surveys, both in the north (NRAO VLA Sky Survey, NVSS, Condon et al. 1998) and in the south (SUMSS, Bock et al. 1999; Mauch et al. 2003), to search for a radio detection. Out of the 33 elusive AGN in the XBS survey only two have been detected in the radio band: one (XBSJ012654.3+191246) has been detected in the NVSS (integrated flux of 1408.1 mJy and peak flux of 947.5 at 1.4 GHz) and the second (XBSJ231546.5-590313) has been detected in the SUMSS (37.3 mJy at 843 MHz). The first source is a radiogalaxy, i.e. it belongs to the so-called "parent-population" of BL Lac objects but the relativistic jets are not aligned with the observer (Galbiati et al. 2005). The second source is the ULIRG IRAS 23128−5919, previously discussed, whose radio emission is likely due to the intense star-formation.

In conclusion we have not found any good BL Lac candidate among elusive AGN of the XBS survey. In principle deeper radio follow-up may detect some additional BL Lac candidate, if present. However, unless the actual cosmological properties (e.g. luminosity function, cosmological evolution and $\mathrm{Log}N - \mathrm{Log}S$) of BL Lacs are significantly different from those estimated until now, we do not expect more than ∼2 BL Lacs among the elusive AGN of the XBS survey. Therefore, it is unlikely that the BL Lac hypothesis can offer a viable explanation for the majority of the elusive AGN in the XBS survey.

5. Summary and conclusions

We have studied in detail the 35 objects in the XBS survey whose optical spectrum is dominated by the light from the host-galaxy and it does not reveal the presence of an AGN (20 objects), or its presence is only suggested (15 objects). In the former group we have both objects showing an early-type galaxy spectrum (11 objects), and objects with an optical spectrum characterized by narrow emission lines with relative intensities suggesting star-formation and/or a LINER classification (9 objects). The latter group includes sources where the presence of an AGN is suggested by some indicators like a possibly broad ($FWHM > 1000$ km s^{-1}) Hα (10 objects) or a (relatively) strong [OIII]λ5007 Å and no Hβ detected (5 objects).

We have used the X-ray spectral analysis, based on *XMM-Newton* epic data 1) to detect the AGN (if present); 2) to classify the sources into absorbed ($N_H > 4 \times 10^{21}$ cm^{-2}) and unabsorbed (or weakly absorbed, $N_H < 4 \times 10^{21}$ cm^{-2}) AGNs. The limit on N_H chosen to discriminate between absorbed and unabsorbed AGN has been fixed in order to match the optical

classification into type 2 and type 1 AGN adopted in the XBS survey (Caccianiga et al. 2007, in prep.), that corresponds to $A_V \sim 2$ mag. We have then studied the origin of the optical "dullness" in those sources in which the presence has been assessed by the X-ray analysis. We summarize the main conclusions.

- The X-ray spectral analysis of the 35 objects has indicated the presence of an AGN in 33 out of 35 sources. This means that, at the flux limit of the XBS survey ($\sim 10^{-13}$ erg s^{-1} cm^{-2}) 11% of the AGN is highly contaminated by the star-light from the host galaxy (elusive AGN) at a level that the correct optical classification of the source (or even the detection of the AGN) is difficult or impossible.;
- The importance of this "recognition problem" is largely dependent on the X-ray luminosity (Fig. 5) and it increases going from X-ray luminous objects ($L_X > 10^{44}$ erg s^{-1}), only slightly affected by this problem (1.5%), to objects with "intermediate" X-ray luminosity (10^{43}–10^{44} erg s^{-1}), where the percentage of elusive sources becomes significant (∼14%) and to sources with low X-ray luminosity (<10^{43} erg s^{-1}), where the recognition problem affects more than 60% of the sources. This result suggests that the recognition problem is mainly due to the global weakness of the source rather than to a particular optical "dullness" (in respect to the X-ray luminosity) of the AGN at least for X-ray luminosities below $\sim 10^{43}$ erg s^{-1}. For luminosities >10^{43} erg s^{-1} also the absorption plays an important role which becomes dominant for luminosities above 10^{44} erg s^{-1};
- The recognition problem affects most, in percentage, type 2 AGN (∼40% are elusive) while it is less important for type 1 AGN (8% are elusive). Given the larger number of type 1 AGN in our samples (even in the HBSS sample), however, most (∼57%) of the elusive AGN in the XBS survey contain a type 1 AGN. Even if we exclude from the analysis those elusive AGN for which some hint for the presence of an AGN can be inferred from the optical spectrum (e.g. those sources with a possibly broad Hα and the sources with a strong [OIII]λ5007 Å emission line) the number of type 1 AGN among the elusive AGN remains significant (50%);
- We have tested the possibility that a Compton-thick AGN is hiding in some of the elusive sources of the XBS survey. To this end we have computed the Compton-thickness parameter, T, defined as the ratio of the X-ray and the [OIII]λ5007 Å flux. No evident Compton-thick candidates have been found although we cannot completely rule out this hypothesis for two sources;
- We have used a simple spectral model, composed by an AGN and host-galaxy template, to better study the elusive AGNs. Using this model, we have shown that for values of AGN/galaxy luminosity ratios (measured at 4050 Å and through the spectrograph slit) above 3, the AGN can be easily recognized in the optical in the large majority of cases (95%) while, for values below 3, the problem of star-light dilution makes the optical AGN detection and/or classification difficult or impossible for a large fraction (55%) of the sources;
- By studying the relation between the X-ray luminosity and the [OIII]λ5007 Å luminosity (which is an indicator of the intrinsic optical luminosity of the AGN) we find that the elusive AGN do not show evidence for $L_X/L_{[OIII]}$ ratios or X-ray-to-optical spectral indices (α_{OX}) significantly different from those observed in non-elusive AGN. Therefore, at the relatively brigth X-ray fluxes sampled by the XBS survey we do not find the "extreme" types of XBONG selected at fainter fluxes by Cocchia et al. (2007) showing high values of $L_X/L_{[OIII]}$ ratios.
- Using the available radio data we have not found any BL Lac candidate among the 33 elusive AGN. Given the X-ray flux limit of the sample and its sky coverage and using the current knowledge on the BL Lac sky-density, we conclude that at most 2 elusive AGN may turn out to be low-luminosity BL Lac objects. The predicted number may be different if the actual statistical properties of BL Lacs will turn out to be significantly different from our current best estimates.

Based on these results, we conclude that the main reason why an important fraction of the AGN appears elusive in the XBS survey is the global strength of the AGN, coupled in some cases with the presence of absorption, and it is not necessary to invoke the explanations ("non-standard" AGN or an additional extra-nuclear absorption within the host-galaxy) that have been proposed to account for objects (typically XBONGs) selected at fainter X-ray fluxes.

We finally stress that the increasing importance of the AGN "recognition problem" with the decreasing of the X-ray luminosity is a factor that must be taken into account when deriving the statistical properties of the AGN (e.g. the luminosity function, the cosmological evolution, ...) as a class and, more importantly, when divided into the subclasses of (optically) absorbed and unabsorbed AGN. This is particularly critical for deep X-ray surveys.

Acknowledgements. We acknowledge helpful discussions with S. Andreon, F. Cocchia, M.J. Marchã and G. Trinchieri. We thank the referee for useful suggestions and a quick review. Based on observations made with: ESO Telescopes at the La Silla Observatories under programme IDs: 070.A-0216, 074.A-0024, 076.A-0267; the Italian Telescopio Nazionale Galileo (TNG) operated on the island of La Palma by the Fundación Galileo Galilei of the INAF (Istituto Nazionale di Astrofisica) at the Spanish Observatorio del Roque de los Muchachos of the Instituto de Astrofisica de Canarias; the German-Spanish Astronomical Center, Calar Alto (operated jointly by Max-Planck Institut für Astronomie and Instututo de Astrofisica de Andalucia, CSIC). A.C., R.D.C., T.M. and P.S. acknowledge financial support from the Italian Space Agency (ASI), the Ministero dell'Università e della Ricerca (MIUR) over the last years. This research has made use of the NASA/IPAC Extragalactic Database (NED) which is operated by the Jet Propulsion Laboratory, California Institute of Technology, under contract with the National Aeronautics and Space Administration. The research described in this paper has been conducted within the *XMM-Newton Survey Science Center* (SSC, see `http://xmmssc-www.star.le.ac.uk`) collaboration, involving a consortium of 10 institutions, appointed by ESA to help the SOC in developing the software analysis system, to pipeline process all the *XMM-Newton* data, and to exploit the *XMM-Newton* serendipitous detections.

References

Bassani, L., Dadina, M., Maiolino, R., et al. 1999, ApJS, 121, 473
Bock, D. C.-J., Large, M. I., & Sadler, E. M. 1999, AJ, 117, 1578
Browne, I. W. A., & Marcha, M. J. M. 1993, MNRAS, 261, 795
Brusa, M., Comastri, A., Mignoli, M., et al. 2003, A&A, 409, 65
Bruzual, G., & Charlot, S. 2003, MNRAS, 344, 1000
Caccianiga, A., Severgnini, P., Braito, V., et al. 2004, A&A, 416, 901
Calzetti, D., & Heckman, T. M. 1999, ApJ, 519, 27
Cardelli, J. A., Clayton, G. C., & Mathis, J. S. 1989, ApJ, 345, 245
Cocchia, F., Fiore, F., Vignali, C., et al. 2006, [arXiv:astro-ph/0612023]
Comastri, A., Mignoli, M., Ciliegi, P., et al. 2002, ApJ, 571, 771
Comastri, A., Brusa, M., Mignoli, M., & the HELLAS2XMM team 2003, Astron. Nachr., 324, 28
Condon, J. J., Cotton, W. D., Greisen, E. W., et al. 1998, AJ, 115, 1693
Della Ceca, R., Pellegrini, S., Bassani, L., et al. 2001, A&A, 375, 781
Della Ceca, R., Maccacaro, T., Caccianiga, A., et al. 2004, A&A, 428, 383
Elvis, M., Schreier, E. J., Tonry, J., Davis, M., & Huchra, J. P. 1981, ApJ, 246, 20

Elvis, M., Wilkes, B. J., McDowell, J. C., et al. 1994, ApJS, 95, 1
Fabbiano, G., & White, N. E. 2006, Compact stellar X-ray sources, 475
Fiore, F., Brusa, M., Cocchia, F., et al. 2003, A&A, 409, 79
Franceschini, A., Braito, V., Persic, M., et al. 2003, MNRAS, 343, 1181
Francis, P. J., Hewett, P. C., Foltz, C. B., et al. 1991, ApJ, 373, 465
Fukazawa, Y., Makishima, K., & Ohashi, T. 2004, PASJ, 56, 965
Galbiati, E., Caccianiga, A., Maccacaro, T., et al. 2005, A&A, 430, 927
Gehrels, N. 1986, ApJ, 303, 336
Georgantopoulos, I., & Georgakakis, A. 2005, MNRAS, 358, 131
González-Martín, O., Masegosa, J., Márquez, I., Guerrero, M. A., & Dultzin-Hacyan, D. 2006, A&A, 460, 45
Griffiths, R. E., Georgantopoulos, I., Boyle, B. J., et al. 1995, MNRAS, 275, 77
Ho, L. C., Filippenko, A. V., & Sargent, W. L. 1995, ApJS, 98, 477
Ho, L. C., Filippenko, A. V., & Sargent, W. L. W. 1997, ApJS, 112, 315
Hornschemeier, A. E., Brandt, W. N., Garmire, G. P., et al. 2001, ApJ, 554, 742
Kewley, L. J., Heisler, C. A., Dopita, M. A., & Lumsden, S. 2001, ApJS, 132, 37
Kim, D.-W., & Fabbiano, G. 2004, ApJ, 611, 846
Liu, J.-F., & Bregman, J. N. 2005, ApJS, 157, 59
Maccacaro, T., Gioia, I. M., Schild, R., Maccagni, D., & Stocke, J. T. 1987, in Proc. Observational Evidence of Activity in Galaxies, IAU Symp., 121, 469
Maiolino, R., & Rieke, G. H. 1995, ApJ, 454, 95
Maiolino, R., Comastri, A., Gilli, R., et al. 2003, MNRAS, 344, L59
Marcha, M. J. M., & Browne, I. W. A. 1995, MNRAS, 275, 951
Marchã, M. J., Caccianiga, A., Browne, I. W. A., & Jackson, N. 2001, MNRAS, 326, 1455
Mason, K. O., Carrera, F. J., Hasinger, G., et al. 2000, MNRAS, 311, 456
Matsushita, K., Makishima, K., Awaki, H., et al. 1994, ApJ, 436, L41
Mauch, T., Murphy, T., Buttery, H. J., et al. 2003, MNRAS, 342, 1117
Moran, E. C., Filippenko, A. V., & Chornock, R. 2002, ApJ, 579, L71
Page, M. J., Loaring, N. S., Dwelly, T., et al. 2006, MNRAS, 369, 156
Perlman, E. S., Madejski, G., Georganopoulos, M., et al. 2005, ApJ, 625, 727
Rigby, J. R., Rieke, G. H., Donley, J. L., Alonso-Herrero, A., & Pérez-González, P. G. 2006, ApJ, 645, 115
Roberts, T. P., & Warwick, R. S. 2000, MNRAS, 315, 98
Severgnini, P., Caccianiga, A., Braito, et al. 2003, A&A, 406, 483
Yuan, F., & Narayan, R. 2004, ApJ, 612, 724
Veilleux, S., & Osterbrock, D. E. 1987, ApJS, 63, 295
Wolter, A., Gioia, I. M., Maccacaro, T., Morris, S. L., & Stocke, J. T. 1991, ApJ, 369, 314
Zhou, H., Wang, T., Yuan, W., et al. 2006, ApJS, 166, 128

Online Material

Appendix A: The reliability of the fluxes derived from the optical spectra

The optical spectra of the XBS sources have been taken with the primary aim of deriving the spectral classification and the redshift. Since both quantities do not require a reliable absolute calibration the observing runs are not necessarily carried out under photometric conditions. In spite of this, for the elusive AGN described in this paper, the [OIII]λ5007 Å flux gives important pieces of information to assess the nature of these objects. In this section we briefly explain how we have estimated the reliability of the fluxes derived from the optical spectra and how we have implemented statistical corrections to minimize the (systematic) errors on the absolute calibration of the spectra.

Several facts may affect the absolute calibration of an optical spectrum. The most important ones are 1) the sky transparency when the objects and the standard star are observed; 2) the seeing conditions with respect to the slit width used during the night; 3) the flux loss across the slit for extended targets. A worsening of the sky transparency and/or the seeing produces a systematic flux loss if it happens during the observation of the source while it produces a systematic increment of the computed fluxes if it happens during the observation of the standard star. The flux loss across the slit in extended targets only affects the host galaxy emission and not the nuclear emission like, for instance, the nuclear [OIII]λ5007 Å flux. The "a posteriori" correction of all these parameters is not trivial. A possible solution could be a renormalization of each spectrum with the photometric points obtained independently. The problems connected with this procedure are: 1) the magnitudes available for the XBS sources are typically taken from APM and are affected by a large uncertainty (≈0.5 mag) and 2) the elusive sources are, by definition, extended sources and, thus, in order to re-normalize the spectrum to the photometric point we need to estimate the fraction of light from the galaxy lost because of the limited size of slit. Given these two main difficulties we decided to adopt a statistical approach using the point-like objects (for which the latter effect is not important) and comparing the fluxes measured from the spectra to the fluxes estimated from the magnitudes. In particular we compute the global spread and any possible systematic shifts using the point-like sources in each of the observing run. We then apply a systematic correction to the spectra of those runs where a significant shift is measured and compute the global spread of the final distribution. In Fig. A.1 we show the results of this analysis i.e. the histogram of the ratio between the 2 fluxes (computed from the spectra and estimated from the *R* magnitude) before and after the systematic corrections on each observing run. The final spread, after the correction is $\sigma = 0.30$. This spread includes both the uncertainties on the spectral fluxes and the errors on the magnitudes ($\sigma_{\rm mag} \sim 0.2$) used for the analysis. The intrinsic spread on the spectral fluxes is then given by:

$$\sigma_{\rm Logflux} = \sqrt{\sigma^2 - \sigma^2_{\rm mag}} \sim 0.22$$

Which corresponds to a relative error on the fluxes of about 50%. The points plotted in all the figures including the [OIII]λ5007 Å fluxes or luminosities are corrected with the systematic shifts discussed above and the reported error bars correspond to the value of $\sigma_{\rm Logflux}$.

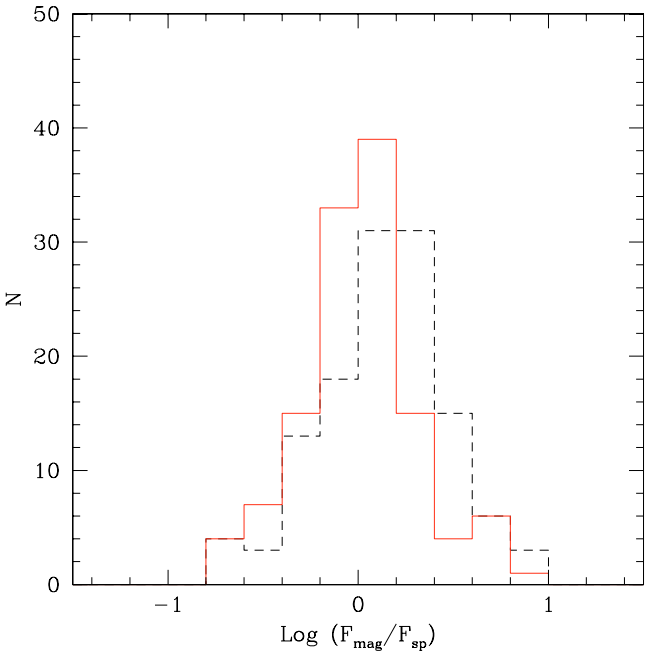

Fig. A.1. The distribution of the ratio between the fluxes at 6400 Å estimated from the *R* magnitude and the ones computed from the optical spectra of the point-like objects before (dotted line) and after (continuous line) the systematic corrections applied to the sources in each observing run.

Appendix B: Notes on individual sources

XBSJ100032.5+553626. The optical classification of this object is controversal in the literature: from the one hand it has been classified as Seyfert 2 by Mason et al. (2000) and, on the other hand, it has been included in a list of ∼2000 NLSy1 extracted from the SDSS by Zhou et al. (2006). The SDSS optical spectrum shows strong emission lines on a blue continuum (the 4000 Å break is =7 ± 5%). The widths of the permitted lines (e.g. the Hβ) are very small (<400 km s^{-1}) and much narrower than the narrowest permitted lines observed in the NLSy1 of the XBS survey (the Hβ widths of the NLSy1 in the XBS survey range from 900 to 1800 km s^{-1}, Caccianiga et al. 2007, in prep.). Additionally the strenght of the FeIIλ4570 Å normalized to the Hβ line (the R_{4570} parameter) is lower (0.28, Zhou et al. 2006) than what is usually observed in NLSy1 (typically $R_{4570} > 0.50$, e.g. Véron-Cetty et al. 2001). Finally, the images taken from the SDSS clearly show an extended source without obvious indication of a strong nucleus. For all these reasons we do not adopt the NLSy1 classification and we prefer a classification as starburst. Indeed, the critical line ratios ([OIII]λ5007 Å/Hβ and [NII]λ6583/Hα) put the source in the starburst/AGN+starburst composite spectrum region in the Veilleux & Osterbrock (1987) diagnostic plot.

XBSJ143911.2+640526 . This source has a "passive" optical spectrum with a relatively low 4000 Å break (33 ± 7%). The lack of emission lines coupled with the reduced break is suggestive of the presence of a significant featureless nuclear emission. Therefore we first tentatively classified of this source as a BL Lac object candidate (Della Ceca et al. 2004). However the shape of the optical spectrum is not very well determined due to the bad observing conditions (cloudy night) and the lack of a standard star observed during the same night. Moreover the observed value of 4000 Å can still be consistent with those observed in elliptical galaxies. Therefore we consider this object as "elusive" AGN candidate and used the X-ray analysis to find and characterize the hidden AGN. The X-ray spectral analysis has revealed the presence of an absorbed AGN ($N_{\rm H} = 2 \times 10^{23}$ cm^{-2}).

The X-ray spectrum is not consistent with the BL Lac hypothesis due to the large column density. These sources, in fact, usually show 0.5–10 keV spectra characterized by unabsorbed or slightly (a few 10^{21} cm^{-2}) absorbed PL (e.g. Perlman et al. 2005) which can be alternatively fit with a model with an intrinsic curvature. Additionally, this source has not been detected in the radio (in the NVSS survey) something that can be considered as a further indication (although not conclusive, see discussion in Sect. 4) against the BL Lac hypothesis. We therefore classify the source as type 2 AGN.